Journal of
Synchrotron
Radiation

ISSN 0909-0495

Received 8 June 2004
Accepted 3 January 2005

Local structure fluctuations as a signature of an inhomogeneous ground state in high-T_c superconductors

J. Mustre de Leon,[a]* M. Acosta-Alejandro,[a] S. D. Conradson[b] and A. R. Bishop[c]

[a]Departamento de Física Aplicada, Cinvestav-Mérida, Yucatán 97310, Mexico, [b]Structure and Properties Group, Los Alamos National Laboratory, Los Alamos, NM 87545, USA, and [c]Theoretical Division, Los Alamos National Laboratory, Los Alamos, NM 87545, USA.
E-mail: mustre@mail.cinvestav.mx

In-plane polarized Cu *K*-edge XAFS on $La_2CuO_{4.1}$ is presented, which indicates a radial in-plane Cu–O distribution function that is not a single Gaussian. Fits to the isolated Cu–O XAFS signal show the presence of a two-site radial distribution function, similar to that found in other La-based cuprate superconductors at temperatures below the temperature associated with the pseudogap appearance, T^*. The appearance of the two-site distribution is interpreted as evidence of a non-homogeneous ground state, preceding the superconducting transition. Similar results found in other copper-oxide superconductors indicate that this non-homogeneous ground state is a general feature of these materials.

Keywords: XAFS; high-T_c superconductors; radial distribution function; inhomogeneous ground state.

1. Introduction

A decade after the discovery of high-temperature copper-oxide superconductors, nuclear magnetic resonance experiments suggested that the charge distribution on these systems was not homogeneous (Hammel & Scalapino, 1996). More recently, tunneling experiments (Derro *et al.*, 2002; Lang *et al.*, 2002) have shown that doped cuprate superconductors indeed exhibit spatial inhomogeneities in the electronic charge distribution on a scale of 10–20 Å. An important question is whether these electronic inhomogeneities are accompanied by an inhomogeneous atomic structure. An inhomogeneous structure on this length scale is expected to produce exotic lattice dynamical properties such as the existence of localized phonon modes and strong coupling between the lattice and charge degrees of freedom, leading to polaron formation. These properties could be key elements in the understanding of the origin of high superconducting transition temperatures in these oxides.

Although diffraction studies on copper-oxide materials showed evidence for macroscopic phase separation in some systems like $La_2CuO_{4+\delta}$, with $0.02 < \delta < 0.06$ (Radaelli *et al.*, 1993), diffraction experiments for materials with the highest superconducting transition temperatures found no evidence of deviation from the average crystalline structure (Radaelli *et al.*, 1993). However, local structural techniques such as X-ray absorption fine structure (XAFS) and pair distribution function (PDF) analysis of diffraction data showed that the local atomic structure presented significant differences from the average crystalline structure (Mustre de Leon *et al.*, 1990; Bianconi *et al.*, 1991; Egami *et al.*, 1991). These results suggested that the atomic structure also presented inhomogeneities on a scale of a few angstroms. After the observation of striped ordered structures on this length scale in other metal oxides, *e.g.* La_2NiO_4, La_2MnO_4 and related compounds (Tranquada, 1994; Chen & Cheong, 1996), the idea of a non-homogeneous lattice structure in copper oxides gained more acceptance. However, the role played by an inhomogeneous ground state in high-temperature superconductivity is not yet clear, as this characteristic is shared with other metal oxides that do not exhibit high-temperature superconductivity.

Regarding the specific nature of the inhomogeneous ground state in La-based copper-oxide superconductors, XAFS experiments have shown the presence of two different in-plane Cu—O bond lengths for temperatures below the characteristic temperature of a pseudogap formation, T^*, in Sr-doped (Bianconi *et al.*, 1996), Nd-doped (Saini *et al.*, 2001) and oxygen-doped La_2CuO_4 (Lanzara *et al.*, 1997). These results have been interpreted within a model in which there are regions of the material which exhibit significant distortions with respect to the average crystalline structure, while other regions present a local structure similar to the average crystalline structure. The length scale of these regions is of the order of 15 Å. These two regions lead to the observation of two different Cu—O distances. However, other XAFS experiments in similar systems like $La_{2-x-y}Sr_x(Eu,Nd)_yCuO_4$

(Niemøller *et al.*, 1998) and $La_{2-x}Ba_xCuO_4$ (Haskel *et al.*, 2000) did not report evidence of a two-site distribution, probably due to the inherent low spatial resolution of XAFS. In this work we address the nature of the in-plane Cu—O pair distribution below T^* in $La_2CuO_{4.1}$.

2. Experimental procedure and data analysis

Sample preparation will be described in detail elsewhere (Conradson *et al.*, 2005). We used a powder sample with a nominal composition $La_2CuO_{4.1}$. This sample consisted of a single macroscopic phase with a superconducting transition temperature of $T_c = 41$ K. This is the highest superconducting transition temperature achieved in oxygen-doped La_2CuO_4. The powder sample was magnetically oriented in epoxy (Mustre de Leon, Conradson *et al.*, 1992). Measurements on this oriented powder sample were carried out at beamline 2-3 of the Stanford Synchrotron Radiation Laboratory (SSRL). XAFS were measured in transmission mode at temperatures $T = 10$, 20, 30 and 100 K. In these measurements we deliberately chose temperatures away from the superconducting transition temperature in order to eliminate any possible effect of such a transition on the local structure of the material. A detailed study on the behavior of the local structure in the vicinity of the superconducting transition temperature will be presented elsewhere. Three scans were recorded at each temperature. The Cu K edge was calibrated using the first inflection point of Cu foil, defined as 8980.3 eV. E_0 was set equal to the calibration energy such that the photoelectron wavevector magnitude is $k = [2m(E - E_0)/\hbar]^{1/2}$. The XAFS signal was extracted using standard procedures (Lee, 1981). Fits to the total XAFS signal were performed using the first three crystallographic shells, corresponding to the Cu—O, Cu—La and Cu—Cu pairs, in the region $3.0 < k < 16.9$ Å^{-1} based on the standard XAFS formula, including multiple-scattering contributions,

$$\chi(k) = -\sum_i S_0^2 N_i \,\mathrm{Im}\frac{\exp(2ikR_i) f_{\mathrm{eff}}(kR_i)}{kR_i^2}\exp\left(2\sigma_i^2 k^2\right). \quad (1)$$

Here, N_i is the number of atoms in the corresponding shell, R_i is the average bond length, σ_i is its root-mean-square fluctuation and S_0 is a many-body reduction factor, which can be estimated from *ab initio* calculations. The complex scattering factors, $f_{\mathrm{eff}}(kR_i)$, were calculated using the *ab initio* simulation code *feff* (Ankudinov *et al.*, 1998). For each shell, N_i was fixed to the average crystallographic value, and R_i and σ_i were allowed to vary at each temperature. S_0 and E_0 were allowed to vary to fit the spectra at $T = 100$ K, and subsequently fixed for fits at other temperatures. Fits on the isolated Cu—O XAFS contribution were performed over the range $4.7 < k < 15.8$ Å^{-1} in order to minimize distortions from the Fourier filtering. In fits performed using a single-Gaussian Cu—O radial distribution function (RDF), R and σ were used as fitting parameters, fixing N, E_0 and S_0 to the values used in the fit to the total XAFS signal. In order to model a non-Gaussian RDF, we used the approach proposed by Mustre de Leon, Conradson *et al.* (1992). In this approach a RDF, $g(z)$, is derived from a model one-dimensional potential, $V(z)$, defined in terms of parameters, which are determined by fitting the modeled XAFS signal to the spectra. If the physical origin of the RDF is dynamic, then $g(z)$ is given in terms of the single-particle wavefunctions and eigenenergies derived from the model potential. In this case we used a double-well potential, $V(z) = a(z - z_1)^2$ for $z < 0$; $V(z) = b(z - z_2)^2$ for $z > 0$. For this two-site minima potential the difference between the first-excited-state and the ground-state energies will yield an estimate of the time scale of the dynamic fluctuations between different bond-length configurations. Fits using a non-Gaussian RDF were performed over the same range as the Gaussian RDF fits, using as fitting parameters the potential curvature parameters a and b, and the potential minima positions z_1 and z_2.

3. Results and discussion

To proceed with the characterization of the Cu—O bond distribution the Cu—O XAFS signal was isolated. To achieve this, the XAFS spectra were fitted in k space using the contributions from the Cu—O, Cu—La and Cu—Cu crystallographic shells in the region $3.0 < k < 16.9$ Å^{-1}. In order to generate the amplitude and phase factors used in this fit, the La_2CuO_4 average crystalline structure was used. The fits reproduce well the Cu—La and Cu—O—Cu contributions, and the obtained structural parameters are in good agreement with diffraction results (Radaelli *et al.*, 1993). However, there is a significant difference between the data and the fit for the Cu—O shell suggesting a deviation of the local Cu—O bond distribution from the Gaussian distribution inferred from crystallographic data (see Fig. 1). The Cu—O signal was then isolated through a Fourier filtering procedure, removing the contributions from farther-away neighbors. Fits to this isolated signal using a single-Gaussian Cu—O RDF show significant

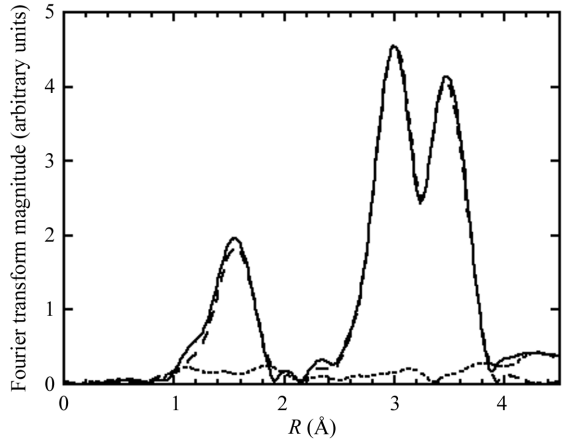

Figure 1
Fourier transform of Cu K-edge XAFS data on $La_2CuO_{4.1}$ at 10 K (solid line), fit based on a Gaussian RDF of Cu—O bonds (dashed line), and difference between data and fit (dotted line). Note the increased difference between data and fit in the region associated with the Cu—O pairs.

disagreement with the data at high k, confirming the results of the fits to the raw XAFS signal (see Fig. 2). In order to model a non-Gaussian RDF, which could be consistent with the spectra, we used the approach outlined above. Fits using a model double parabolic potential (see Fig. 3) similar to that used by Mustre de Leon *et al.* (1990) are consistent with the experimental signal (see Fig. 2). These fits lead to a two-site Cu—O RDF with Cu—O bond distances similar to those found in $La_{1.85}Sr_{0.15}CuO_4$, at temperatures below the pseudogap formation temperature (Bianconi, 1996; Saini, 2001). It is important to note that, given the uncertainties in the XAFS signal at high k, illustrated by the error bars in Fig. 2, it is likely that more complicated distributions are also consistent with the data, as those proposed by Mihailovic & Kabanov (2001). The two-site parabolic potential was chosen as the simplest model beyond a single harmonic site model. It is important to stress that the spatial resolution for XAFS is limited by the highest value of the photoelectron momentum achieved in the experiments, k_{max}. In this case $k_{max} = 15.8$ Å^{-1}, which limits the spatial resolution to distortions larger than 0.09 Å. Hence the inability to discern particular details of the RDF with the available data. We also note that the use of a static potential, although adequate to derive a non-Gaussian RDF consistent with the XAFS data, leads to an incorrect description of higher excited states, yielding excitation energies inconsistent with optical spectroscopy results and incorrect isotopic shifts of these excitations. A many-body model which exhibits polaronic behavior and generates both a RDF consistent with XAFS results and higher excited states consistent with optical and neutron inelastic results has been proposed by Mustre de Leon, Batistic *et al.* (1992).

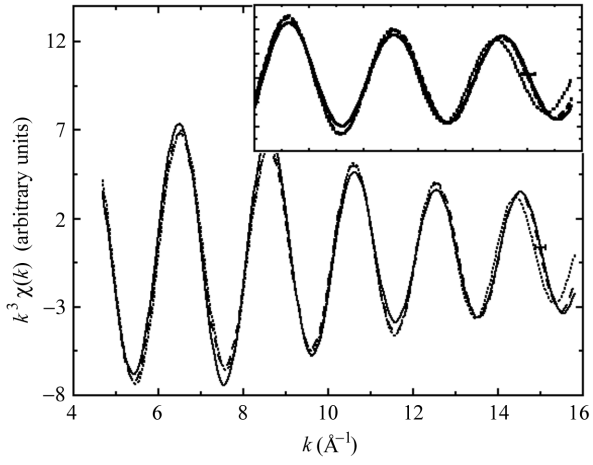

Figure 2
Experimental isolated Cu—O contribution to the Cu K-edge XAFS on $La_2CuO_{4.1}$ at 10 K (solid line), fit based on a RDF of Cu—O bonds derived from a two-site potential, as described in the text (dashed line), and fit based on a Gaussian RDF of Cu—O bonds (dotted line). Note the increased deviation between the Gaussian RDF fit and data at high values of k. Inset: detail of the fits and data in the region $10 < k < 16$ Å^{-1}.

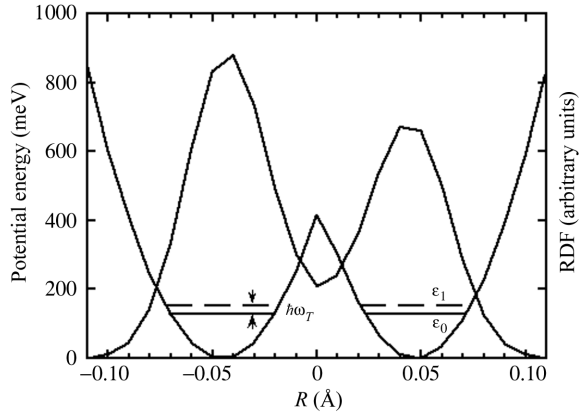

Figure 3
Two-site potential and Cu—O RDF derived from fits to the copper in-plane oxygen XAFS at 20 K. The ground-state and first-excited-state energies are also shown. The quantity $\hbar\omega_T = \varepsilon_1 - \varepsilon_0$ corresponds to the tunneling frequency between the two potential minima.

An explanation for the origin of the RDF obtained could be the presence of local lattice distortions introduced by the oxygen dopant atoms. However, nuclear magnetic resonance experiments have shown that the existence of two copper sites, which have a different local neighborhood, is not related to the presence of distortions caused by dopants, but rather due to the presence of doped holes in the planes, independently of the doping mechanism to introduce these holes (see, for example, Hammel *et al.*, 1993). We also note that two-site distributions similar to the ones we found in $La_2CuO_{4.1}$ are present in $La_{1.85}Sr_{0.15}CuO_4$ (Bianconi, 1996; Saini, 2001), where the distribution of Sr dopants is different from the distribution of extra O atoms found in $La_2CuO_{4.1}$. Another possibility for the origin of this RDF is the presence of an inhomogeneous ground state with dynamical fluctuations such as that proposed by Ovchinnikov *et al.* (2001). Such an inhomogeneous state would appear below the formation of a pseudogap (Bianconi *et al.*, 1996).

The RDF at the highest measured temperature (100 K) is not as sharp as that at low temperatures, showing a tendency towards a single Gaussian distribution, as that found for temperatures above the disappearance of a pseudogap.

It is important to note that XAFS cannot distinguish between static and dynamic local distortions, owing to the intrinsic fast time scale of the ejected photoelectron. Other experimental techniques, depending on their intrinsic time scale, might not be able to detect dynamic distortions. Distortions or inhomogeneities which have been observed by scanning tunneling microscopy would be static distortions, given the time scale of the probe. Nuclear magnetic resonance does have a faster time scale, and would be sensitive to dynamical fluctuations which are slow compared with typical phonon time scales. XAFS has a much faster time scale than phonon time scales, and therefore it is able to probe distortions that are either static or dynamic, although it cannot establish whether the distortions are static or dynamic. Neutron inelastic scattering can be tuned to specific time scales and can therefore resolve distortions with different time scales. On the other hand, elastic scattering experiments, like X-ray and neutron diffraction, probe the static correlation function and in principle are only sensitive to static distortions (Salkola *et al.*, 1994).

Under the assumption of a dynamical origin for the observed two-site distribution, a tunneling frequency between the two sites can be extracted as the energy difference between the first excited state and the ground state, $\hbar\omega_T = \varepsilon_1 - \varepsilon_0$. It is interesting to note that the energy difference between the normal (85 meV) and anomalous branch (70 meV) for the longitudinal optical Cu—O mode observed at low temperatures (below T^*) by neutron inelastic scattering (McQueeney *et al.*, 1999) is of the same order as the energy associated with the tunneling at low temperatures ($\sim$16 meV) derived from our fits, supporting the idea of a dynamical origin for the observed RDF. We had found a similar structure of the RDF for the in-plane Cu—O in Tl-based superconductors (Conradson *et al.*, 1997), and for the Cu—O(axial) bond in $YBa_2Cu_3O_7$ (Mustre de Leon *et al.*, 1990). Theoretical many-body models, which generate small polaron formation, also predict the onset of a non-homogeneous ground state below the pseudogap formation temperature (Bishop *et al.*, 2003). Below T^* the individual polarons become thermally stable, forming a polaron liquid of filamentary segments with a very slow polaronic diffusion, but with a much faster internal charge tunneling accompanied by dynamic local lattice distortions like those found in this work. Although currently available data provide evidence for small polarons, they do not distinguish isolated polarons from their anticipated organization into filamentary segments for $T^* > T > T_c$ as precursors to correlated percolation paths for $T < T_c$, which could be responsible for the superconductivity in these materials.

4. Summary

In summary, we conclude that the in-plane Cu—O distribution of bond lengths in $La_2CuO_{4.1}$ found in this study is consistent with a two-site radial distribution function similar to that found in other La-based copper oxides, below the temperature of the pseudogap formation, T^*. This radial distribution is similar to the distributions found in Tl-based copper-oxide superconductors and in $YBa_2Cu_3O_7$. This radial distribution function could arise from the presence of an inhomogeneous structure on the local scale, which has been suggested by other experimental techniques, and seems to be a general feature of copper-oxide superconductors.

XAFS experiments were performed at the Stanford Synchrotron Radiation Laboratory, which is operated by the US Department of Energy. This work is supported in part by CONACYT-Mexico and the US Department of Energy.

References

Ankudinov, A. L., Ravel, B., Rehr, J. J. & Conradson, S. D. (1998). *Phys. Rev. B*, **58**, 7565–7576.
Bianconi, A., Li, C. X., Campanella, F., Dellalonga, S., Pettiti, I., Pompa, M., Turtu, S. & Udron, D. (1991). *Phys. Rev. B*, **44**, 4560–4569.
Bianconi, A., Saini, N. L., Lanzara, A., Missori, M., Rossetti, T., Oyanagi, H., Yamaguchi, H., Oka, K. & Ito, T. (1996). *Phys. Rev. Lett.* **76**, 3412–3415.
Bishop, A. R., Mihailovic, D. & Mustre de Leon, J. (2003). *J. Phys. Condens. Matter*, **15**, L169–L174.
Chen, C. H. & Cheong, S. W. (1996). *Phys. Rev. Lett.* **76**, 4042–4045.
Conradson, S. D., Mustre de Leon, J. & Bishop, A. R. (1997). *J. Superconduct.* **10**, 329–332.
Conradson, S. D., Bishop, A. R. & Mustre de Leon, J. (2005). In preparation.
Derro, D. J., Hudson, E. W., Lang, K. M., Pan, S. H., Davis, J. C., Markert, J. T. & de Lozanne, A. L. (2002). *Phys. Rev. Lett.* **88**, 097002–097006.
Egami, T., Toby, B. H., Billinge, S. J. L., Rosenfeld, H. D., Jorgensen, J. D., Hinks, D. G., Dabrowski, B., Subramanian, M. A., Crawford, M. K., Farneth, W. E. & McCarron, E. M. (1991). *Physica C*, **185**, 867–868.
Hammel, P. C., Reyes, A. P., Cheong, S.-W. & Fisk, Z. (1993). *Phys. Rev. Lett.* **71**, 440–443.
Hammel, P. C. & Scalapino, D. J. (1996). *Philos. Mag. B*, **74**, 573–578.
Haskel, D., Stern, E., Dogan, F. & Moodenbaugh, A. R. (2000). *Phys. Rev. B*, **61**, 7055–7076.
Lang, K. M., Madhavan, V., Hoffman, J. E., Hudson, E. W., Eisaki, H., Uchida, S. & Davis, J. C. (2002). *Nature (London)*, **415**, 412–416.
Lanzara, A., Saini, N. L., Bianconi, A., Hazemann, J. L., Soldo, Y., Chou, F. C. & Johnston, D. C. (1997). *Phys. Rev. B*, **55**, 9120–9124.
Lee, P. A., Citrin, P. H., Eisenberger, P. & Kincaid, B. M. (1981). *Rev. Mod. Phys.* **53**, 769–871.
McQueeney, R. J., Petrov, Y., Egami, T., Yethiraj, M., Shirane, G. & Endoh, Y. (1999). *Phys. Rev. Lett.* **82**, 628–630.
Mihailovic, D. & Kabanov, V. V. (2001). *Phys. Rev. B*, **63**, 054505.
Mustre de Leon, J., Conradson, S. D., Batistic, I. & Bishop, A. R. (1990). *Phys. Rev. Lett.* **65**, 1675–1678.
Mustre de Leon, J., Conradson, S. D., Batistic, I., Bishop, A. R., Raistrick, I. D., Aronson, M. C. & Garzon, F. H. (1992). *Phys. Rev. B*, **45**, 2447–2457.
Mustre de Leon, J., Batistic, I., Bishop, A. R., Conradson, S. D. & Trugman, S. A. (1992). *Phys. Rev. Lett.* **68**, 3236–3239.
Niemøller, T., Buchner, B., Cramm, M., Huhnt, C., Tröger, L. & Tischer, M. (1998). *Physica C*, **299**, 191–196.
Ovchinnikov, Y. N., Wolf, S. A. & Kresin, V. Z. (2001). *Phys. Rev. B*, **63**, 064524.
Radaelli, P. G., Jorgensen, J. D., Schultz, A. J., Hunter, B. A., Wagner, J. L., Chou, F. C. & Johnston, D. C. (1993). *Phys. Rev. B*, **48**, 499–510.
Saini, N. L., Oyanagi, H., Lanzara, A., Di Castro, D., Agrestini, S., Bianconi, A., Nakamura, F. & Fujita, T. (2001). *Phys. Rev. B*, **64**, 132510.
Salkola, M., Bishop, A. R., Mustre de Leon, J. & Trugman, S. A. (1994). *Phys. Rev. B*, **49**, 3671–3674.
Tranquada, J. M., Buttrey, D. J., Sachan, V. & Lorenzo, J. E. (1994). *Phys. Rev. Lett.* **73**, 1003–1006.